Chemical Science

ROYAL SOCIETY OF CHEMISTRY

EDGE ARTICLE

View Article Online
View Journal | View Issue

Cite this: *Chem. Sci.*, 2023, **14**, 4641

All publication charges for this article have been paid for by the Royal Society of Chemistry

Chiral spirosiladiphosphines: ligand development and applications in Rh-catalyzed asymmetric hydrosilylation/cyclization of 1,6-enynes with enhanced reactivity†

Fei Hou,[ab] Minjie Liu,[ab] Tong Ru,[ab] Zequn Tan,[ab] Yingtang Ning *[ab] and Fen-Er Chen *[ab]

Received 17th November 2022
Accepted 24th March 2023

DOI: 10.1039/d2sc06349b

rsc.li/chemical-science

Spirodiphosphines have been successfully applied in various asymmetric catalytic transformations. However, controlling the coordinating conformations by the direct displacement of the spiro atom remains elusive. Herein, we report the application of Si-centered spirodiphosphine (Si-SDP) ligands in the enantioselective hydrosilylation/cyclization of 1,6-enynes. The Si-SDPs showed superior reactivity to existing C2-symmetric diphosphines, allowing the generation of a range of chiral pyrrolidines with high yields and enantioselectivity (up to 96% yield and 92% ee) at room temperature with low catalyst loading. The mechanistic observations were consistent with the modified Chalk–Harrod mechanism, and the high reactivity of Si-SDPs was further leveraged for the room-temperature Rh-catalyzed hydrosilylation of alkynes.

Introduction

Chiral diphosphines with C2 symmetry represent a privileged class of ligands in asymmetric catalysis.[1] These atropos ligands (Fig. 1), exemplified by BINAP (**L1**)[2] and spirodiphosphines (SDPs, **L2**),[3] help to improve catalyst activity and induce enantioselectivity. In particular, SDPs derived from the rigid 1,1′-spirobiindane backbone are extraordinarily successful.[3] The larger bite angles, accompanied by the conformational rigidity and chemical robustness of SDPs,[4] have contributed to tremendous advances in enantioselective transformations, including asymmetric hydrogenation,[5] allylic alkylation,[4b] hydrosilylation/cyclization,[6] and others.[7]

Effective control over the ligand conformation in chelating complexes is considered a key concept for ligand design.[8] Steric modulation of SDPs (**L2**) has primarily relied on the installation of additional substituents, resulting in ligands with various steric properties.[9] On the other hand, as the rotation of the spirocyclic framework is restricted by the tetrahedral structure of the spiro carbon atom, replacing this conjunct atom would provide straightforward access to regulating the conformations. In this context, Wang reported the asymmetric synthesis of spirosilabiindanes by hydrosilylation.[10] This protocol allows for the preparation of monodentate phosphoramidites, which promote asymmetric hydrogenation reactions of olefins and asymmetric intramolecular carboamination reactions.[10a,11] However, diphosphine ligands based on the spirosilabiindanes backbone (Si-SDPs, **L3**) remain unexplored.[21] The elongated C–Si bonds in these ligands should create a robust coordination space distinct from the carbon-centered **L2**. Our preliminary computations suggested that a significantly larger P–M–P bite angle than SDP (**L2**) can be achieved with Si-SDP **L3** (Fig. S1†). We are interested in the effect of such regulated geometry, which is indulgent to the required orbital overlap during various common steps in organometallic chemistry.[12]

In the current study, we chose the Rh-catalyzed asymmetric silylcyclization of 1,6-enynes[13–15] as an optimal reaction to challenge the effect of Si-SDPs (Scheme 1A). This reaction, originally developed by Ojima,[13] is a synthetically useful transformation with the one-step formation of a carbon–carbon bond and a carbon–silicon bond. The asymmetric versions were independently reported by Widenhoefer[17] and Zhou[6] (Scheme 1A). The implementation of C2-symmetric diphosphines,

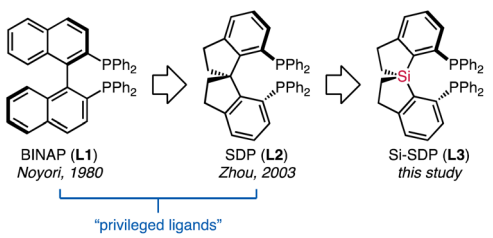

Fig. 1 Examples of C2-symmetric diphosphines.

[a]*Engineering Center of Catalysis and Synthesis for Chiral Molecules, Fudan University, 200433 Shanghai, China. E-mail: ningyt@fudan.edu.cn; rfchen@fudan.edu.cn*

[b]*Shanghai Engineering Center of Industrial Catalysis for Chiral Drugs, 200433 Shanghai, China*

† Electronic supplementary information (ESI) available. CCDC 2213409 and 2220312. For ESI and crystallographic data in CIF or other electronic format see DOI: https://doi.org/10.1039/d2sc06349b

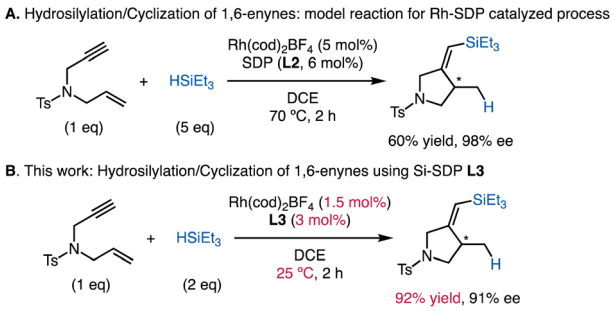

Scheme 1 Rh-catalyzed hydrosilylation/cyclization.

especially Zhou's SDP ligand **L2**, delivered high levels of stereocontrol at 70 °C. However, mild yields and relatively high catalyst loadings (5 mol%) of the reaction limit its further applications. The reaction pathway was assumed to follow a modified Chalk–Harrod mechanism[18] interrupted by β-migratory insertion into the Rh–C bond.[13b] We envisioned that the coordination of **L3** with a large bite angle could accelerate the reductive elimination and migratory insertion steps[12] in the catalytic cycle, as well as favoring the formation of the sterically crowded intermediate required for silylcyclization. Our results demonstrate the superior reactivity of Si-SDPs compared to the corresponding SDPs, affording chiral pyrrolidines[16] that are ubiquitous in natural products and pharmaceuticals at room temperature with low catalyst loadings (Scheme 1B).

Results and discussion

Effect of ligands

To verify the catalyst activity generated from Si-centered spiro diphosphines, we prepared Si-SDPs (**L3–L6**, Table 1) that are

Table 1 Screening of ligands[a]

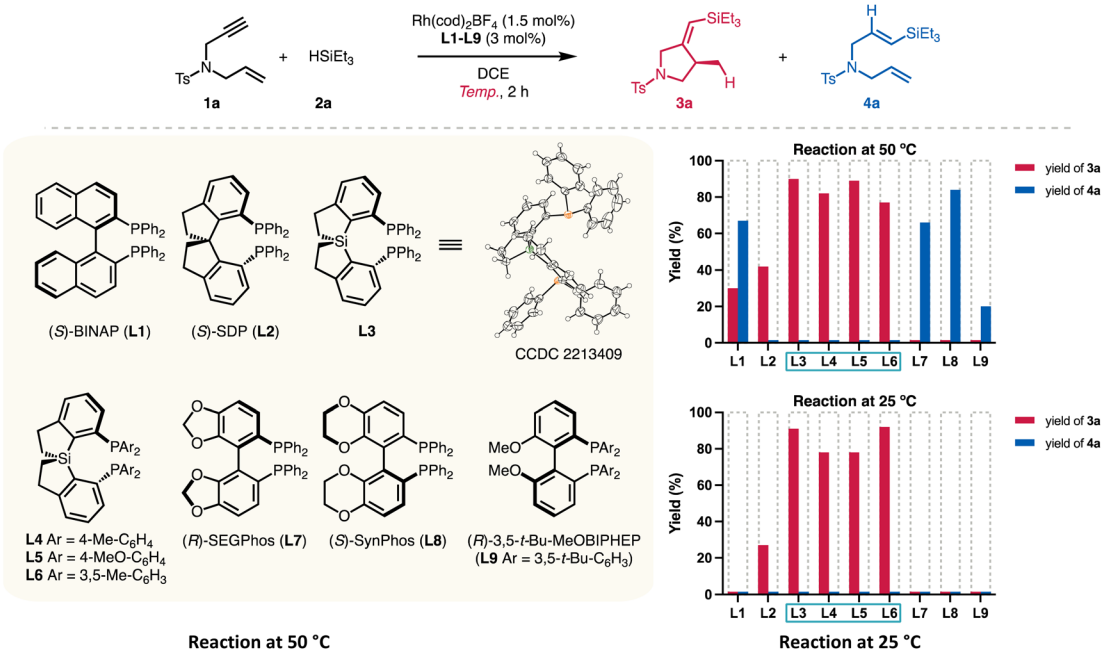

Reaction at 50 °C					Reaction at 25 °C				
		Yield[b] (%)					Yield[b] (%)		
Entry	Ligand	**3a**	**4a**	ee%[c] (**3a**)	Entry	Ligand	**3a**	**4a**	ee%[c] (**3a**)
1	**L1**	30	67	n.d.	10	**L1**	—	—	—
2	**L2**	42	—	95	11	**L2**	27	—	94
3	**L3**	95	—	91	12	**L3**	92	—	91
4	**L4**	82	—	90	13	**L4**	78	—	90
5	**L5**	89	—	89	14	**L5**	78	—	90
6	**L6**	77	—	91	15	**L6**	92	—	89
7	**L7**	—	66	—	16	**L7**	—	—	—
8	**L8**	—	84	—	17	**L8**	—	—	—
9	**L9**	—	20	—	18	**L9**	—	—	—

[a] Reactions were performed with **1a** (0.2 mmol), **2a** (0.4 mmol), $Rh(cod)_2BF_4$ (1.5 mol%), and **L1–L9** (3 mol%) in DCE (2.0 mL). [b] NMR yield using dibromomethane as an internal standard. [c] ee values were determined by chiral HPLC of the desilylated compounds.

relatively air-stable and easy to handle, based on reported procedures[5a] for other diphosphines.

Different diphosphines **L1–L9** were evaluated using the reaction of enyne **1a** and triethylsilane (**2a**) (Table 1). As Zhou reported that SDP **L2** displayed the highest yield (62%) at a reaction temperature of 50 °C,[6] we first examined the performance of **L1–L9** at the same temperature using a reduced amount of $Rh(cod)_2BF_4$ (1.5 mol%). The reaction using BINAP (**L1**) gave a mixture of the cyclized product **3a** (30% yield) and the hydrosilylation product **4a** (67% yield, entry 1). SDP (**L2**) showed good selectivity to silylcyclization, and **3a** was obtained in 42% yield (entry 2). All the tested Si-centered spirodiphosphine ligands gave the desired **3a** in high yields (77–90%) with high ee values (entries 3–6). Ligand **L3**, bearing phenyl groups on the phosphorous atoms, showed the highest yield (95%) and enantioselectivity (91%). Other C2-symmetric ligands **L7–L9** failed to provide the cyclized products. Instead, the hydrosilylation product **4a** was obtained in 20–84% yields (entries 7–9), indicating distinct chemoselectivity and high reactivity enabled by the spirosilabiindane structures.

A stark contrast in catalyst activity arose by lowering the reaction temperature (entries 10–18). Only the ligands **L2–L6** possessing spirocyclic scaffolds promoted the conversions of **1a** at 25 °C. SDP ligand **L2** gave the cyclized product **3a** in 27% yield at room temperature for 2 h (entry 11). On the other hand, full conversion was observed for **L3** at 25 °C, giving **3a** in 92% yield and 91% ee (entry 12). Other spirodiphosphines with a Si center atom (entries 13–15) also allowed the room-temperature silylcyclization reaction to occur with good yields (78–92%) and ee values (89–90% ee). Ligands **L7–L9**, which afforded hydrosilylation product **4a** at 50 °C, exhibited marginal reactivity (entries 16–18).

Reaction scope

The substrate scope of the reaction enabled by the **L3**-modified Rh catalyst is outlined in Scheme 2. Chiral 1-sulfonyl pyrrolidines with different substituents on the sulfonyl groups reacted with $HSiEt_3$ to afford the cyclized products in satisfactory yields. The enantioselectivity of the reaction was determined based on the desilylated products for improved handling. Alkyl (**3b**), chlorine (**3c**), and phenyl (**3d**) groups were well tolerated, and the products were isolated in 90–96% yields. We tested the electron-donating groups (**3e** and **3f**) and electron-withdrawing groups (**3g–3i**) on the phenyl group, and there were no significant electronic effects of these substituents on the reaction yields and enantioselectivity. Including a methyl group (**3j**) or a bromide atom (**3k**) in the *meta*-position of the phenyl ring also results in the corresponding products with good yields. The

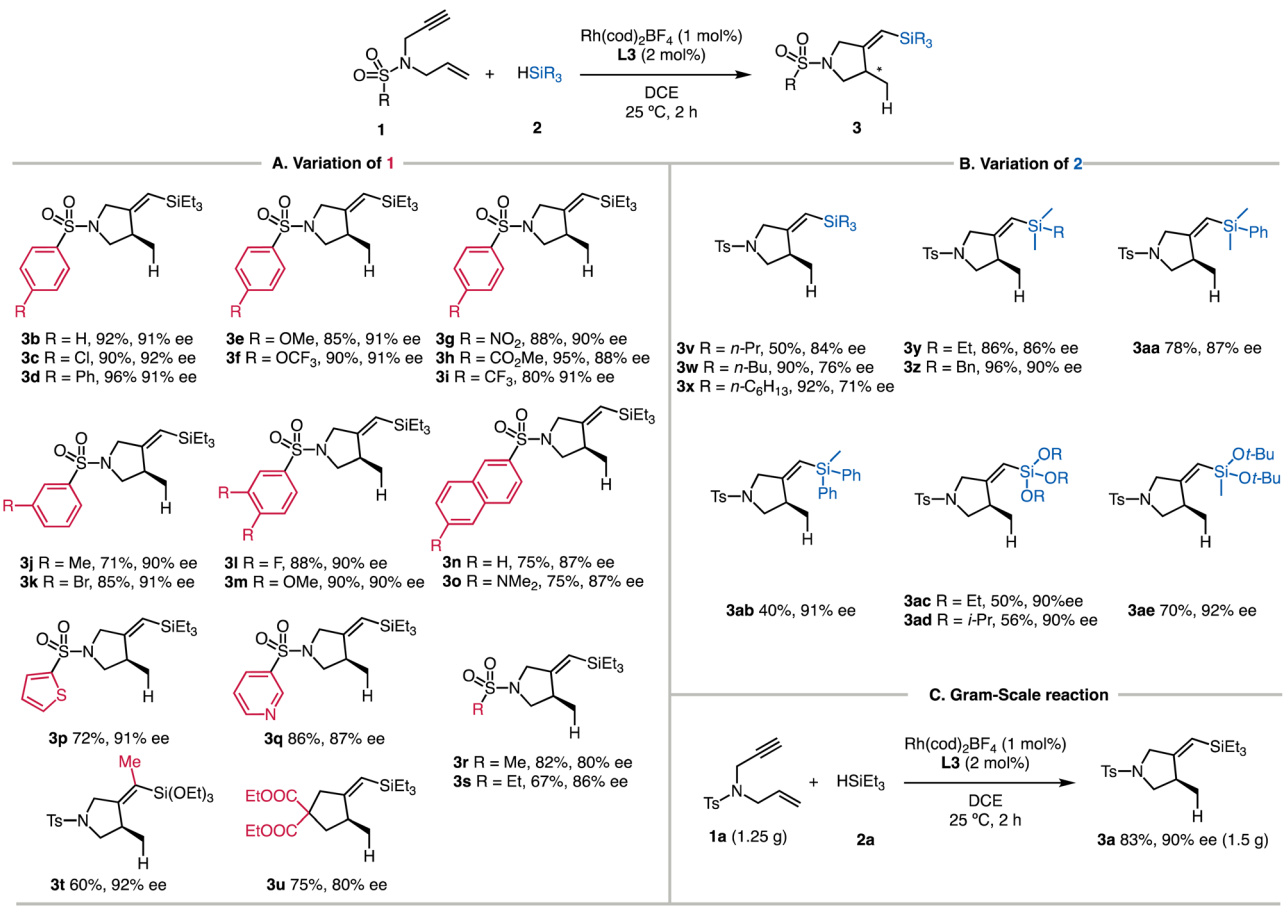

Scheme 2 Scope of Rh-**L3** catalyzed silylcyclization [a–c].[a] Reactions were performed with **1a** (0.2 mmol), **2a** (0.4 mmol), $Rh(cod)_2BF_4$ (1.5 mol%), and **L3** (3 mol%) in DCE (2.0 mL).[b] Yields of isolated **3**.[c] ee values were determined by chiral HPLC of the desilylated compounds.

reductively labile bromide survived under the current conditions. We explored two examples with multiple substituents (**3l** and **3m**), and both reactions proceeded smoothly. Naphthyl-substituted enyne underwent smooth silylcyclization (**3n**, 75% yield, and 87% ee), and comparable yield and selectivity were observed by introducing an additional NMe_2 substituent (**3o**). We also examined several heterocyclic substituents, and both the thiophenyl (**3p**) and pyridyl (**3q**) rings were compatible. The **L3**-modified catalyst was also successfully applied to substrates having aliphatic sulfonyl groups, forming **3r** and **3s** in good yields. We found that the substrate with internal alkynes reacted with triethoxysilane smoothly, affording **3t** in 60% yield and 92% ee. Notably, no conversion was observed between the same enyne (**1a**) with triethylsilane **2a**.The catalyst employing **L3** is also suitable for the asymmetric synthesis of substituted cyclopentanes. The silylcyclization afforded **3u** containing a quaternary carbon atom in 80% ee under the standard reaction conditions.

Using enyne **1a**, we next evaluated the influence of different silanes (Scheme 2B). Different alkyl substitution patterns on the silicon atom (**3v–3z**) posed no difficulty for the reactions. The benzyl group remained intact to deliver **3z** in 96% yield and 90% ee. Attaching a phenyl group to the silicon atom also gave the corresponding **3aa** in 78% yield and 87% ee, but the silane with multiple phenyl groups led to lower reactivity (**3ab**, 40% yield, and 91% ee). Trialkoxysilanes were also applicable, giving the desired **3ac** and **3ad** in moderate yields, which are facile counterparts for coupling reactions (ESI†).[19] Sterically hindered silane also reacted well to generate **3ae**. In order to capitalize on the superior reactivity, the scalability of the developed reaction is illustrated in Scheme 2C. When 1.25 g of **1a** was employed, the silylcyclization with **2a** produced **3a** in 83% yield with 90% ee.

Mechanistic insights

To further probe the high activity of the Si-centered ligand **L3**, we performed several experiments concerning the mechanistic details. The hydrosilylation of alkyne **5** was feasible, but the addition of the H–Si bond to alkene **7** could not operate even at 50 °C (Scheme 3A). Thus, the hydrosilylation/cyclization process is likely triggered by the migratory insertion of the alkyne into the Rh–Si bond (modified Chalk–Harrod mechanism). Among the different Rh species tested, only the cationic $Rh(cod)_2BF_4$ and $Rh(cod)_2OTf$ showed conversions of the substrates (Scheme 3B). HRMS analysis also confirmed the formation of Rh-**L3** and the subsequent coordination of **1a** (Fig. S8†). In addition, we obtained the cryogenic structure of **L3** coordinating with $PdCl_2$ (Scheme 3D). The tailored P–Pd–P bite angle for **L3** (101.0°) is larger than those of BINAP (**L1**, 92.7°) and SDP (**L2**, 96.0°) (Fig. S1†). We hypothesize that this large bite angle of **L3** could be replicated in analogous Rh complexes, which would underlie the high reactivity of **L3**.

The deuterium labeling experiment suggested that the alkyne C–H bond remained intact during the enyne cyclization (Scheme S2†). Moreover, we observed a secondary deuterium kinetic isotope effect (^{2}H KIE) of 1.38 from intermolecular competition experiments (Scheme 3D). Additionally, we measured the initial rates of the reaction by varying the

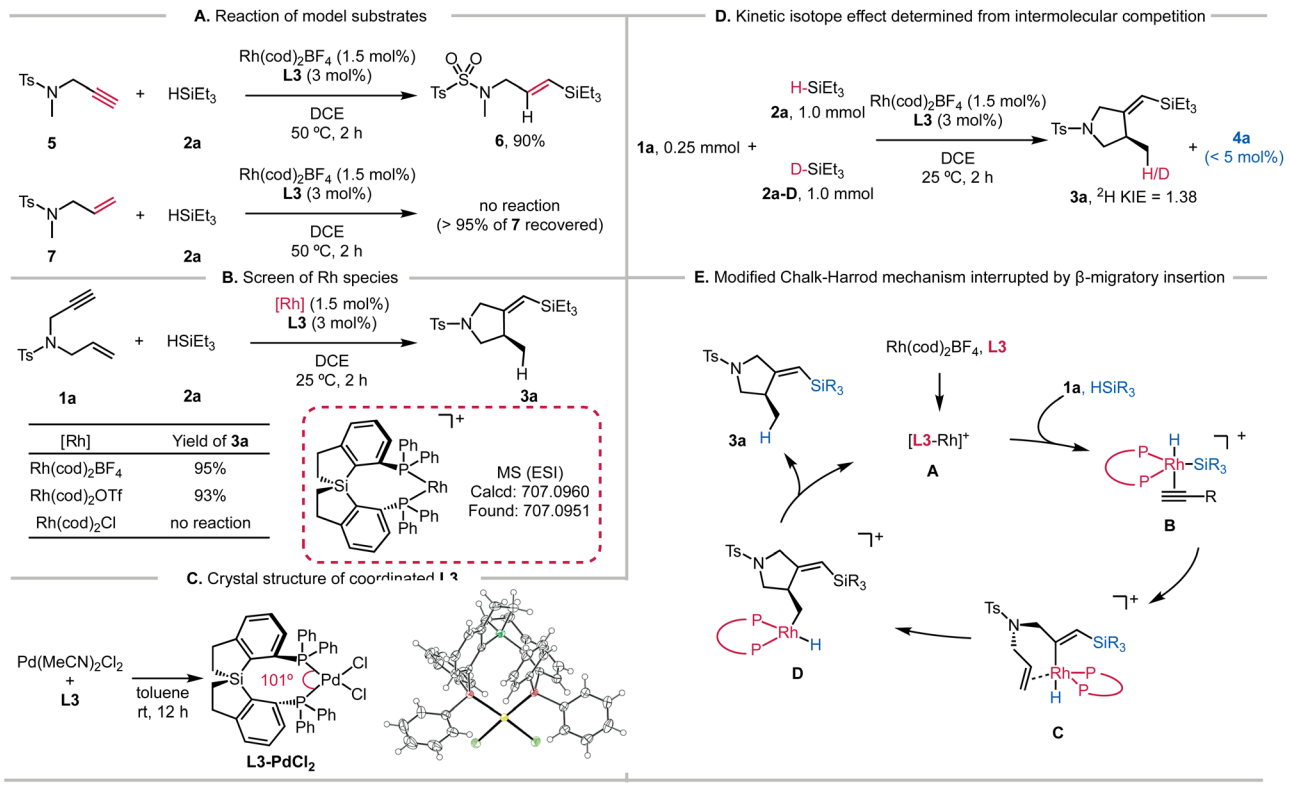

Scheme 3 Mechanistic insights into Rh-**L3** catalyzed silylcyclization.

concentrations of **1a** and **2a**, revealing that the reaction was first order to the concentration of **1a** and zero order to that of **2a** (Fig. S9†). As such, the oxidative addition of the H–Si bond across the cationic Rh species is not involved in the rate-determining step. Interestingly, a marginal amount of hydrosilylation product **4a** was detected with excess $HSiEt_3$ (**2a**) (Scheme 3D). These results are consistent with the catalytic cycle shown in Scheme 3E. Intermediate **A** formed by mixing **L3** and $Rh(cod)_2BF_4$ reacted with silanes in the presence of **1a** to generate intermediate **B**. The migratory insertion of the alkyne into the Rh–Si bond forms intermediate **C**, which is followed by cyclization achieved by the insertion of the alkene into the new Rh–C bond. The resulting Rh-alkyl intermediate **D** having the pyrrolidine skeleton is ready to produce **3a** and regenerate the active Rh species **A** *via* reductive elimination.

Application of Si-SDP to room-temperature hydrosilylation

Finally, we sought to examine the reactivity of Rh/**L3**-catalyzed hydrosilylation of alkynes, given the broad application of this transformation.[20] Room-temperature hydrosilylation of **5** using **L3** produced **6** in a 92% yield within 2 h (Scheme 4A). Using **L2** gave a limited yield of 22% under the same conditions, which supports the superior reactivity of Si-centered **L3** in Rh-catalyzed hydrosilylation. The higher reactivity of Si-SDP (**L3**) in this hydrosilylation process is qualitatively supported by our preliminary DFT calculations, using silane and acetylene as simplified substrates. While such simplifications would underestimate the energy barriers, the computational results suggested that the modified Chalk–Harrold mechanism is viable (Scheme 4B). For the process using SDP (**L2**), oxidative addition of the silane is followed by migratory insertion of the alkyne into the Rh–Si bond. The transition state of this migratory insertion step (TS_C-**2**) has an energy barrier of 8.2 kcal mol^{-1}; whereas, in the reaction employing Si-centered **L3**, the migratory insertion *via* TS_{Si}-**2** is energetically less demanding (5.0 kcal mol^{-1}). The P–M–P angle increased from 100.3° to 101.1° for **L2** and from 107.1° to 111.8° for **L3**. The large bite angle of **L3** would thus accelerate the migratory insertion to enable room-temperature hydrosilylation.

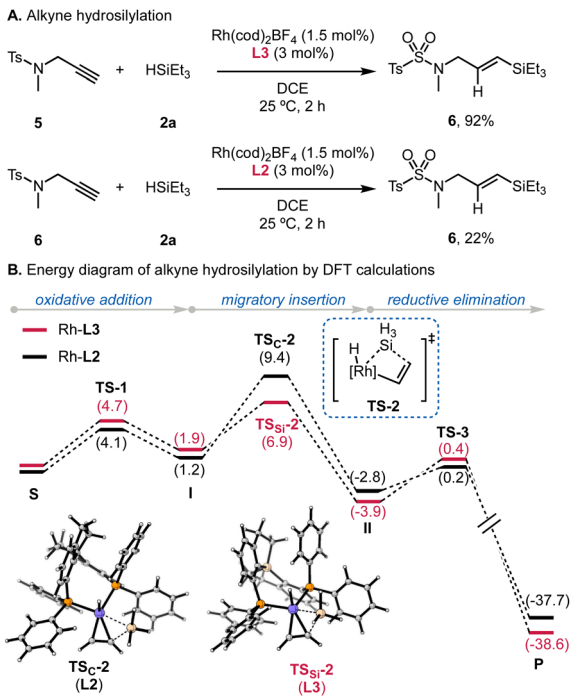

Scheme 4 Room-temperature hydrosilylation of alkynes.

Conclusions

We have synthesized a series of Si-centered spirodiphosphines (Si-SDPs), and their efficiency as ligands in Rh-catalyzed silylcyclization of 1,6-enynes was examined. These Si-SDPs suggested higher reactivity than other C2-symmetric ligands. The reaction tolerates a wide range of substrates, affording cyclized pyrrolidines in high yields and satisfactory enantioselectivity at room temperature. Further experiments revealed the crucial role of Si-SDP in accelerating the catalytic pathway composed of a modified Chalk–Harrod mechanism interrupted by β-migratory insertion. With the Si-centered spiro scaffolds of C2-symmetry, we anticipate that Si-SDPs will find broad applications in asymmetric catalysis.

Data availability

The datasets supporting this article have been uploaded as part of the ESI.†

Author contributions

H. F., Y. N., and F.-E. C. conceived the research. H. F., M. L., T. R., and Z. T. performed the laboratory experiments. H. F. and Z. T. synthesized the ligands. H. F. and Y. N. conducted the DFT calculations. H. F., Y. N. and F. -E. C. prepared the manuscript with feedback from the other authors.

Conflicts of interest

There are no conflicts to declare.

Acknowledgements

Financial support from the National Natural Science Foundation of China (22077018) is gratefully acknowledged.

Notes and references

1 (*a*) T. P. Yoon and E. N. Jacobsen, *Science*, 2003, **299**, 1691–1693; (*b*) Q.-L. Zhou, *Privileged Chiral Ligands and Catalysts*, Wiley-VCH, Weinheim, 2011.
2 A. Miyashita, A. Yasuda, H. Takaya, K. Toriumi, T. Ito, T. Souchi and R. Noyori, *J. Am. Chem. Soc.*, 1980, **102**, 7932–7934.
3 (*a*) S.-F. Zhu and Q.-L. Zhou, *Acc. Chem. Res.*, 2012, **45**, 1365–1377; (*b*) J.-H. Xie and Q.-L. Zhou, *Acc. Chem. Res.*, 2008, **41**, 581–593; (*c*) K. Ding, Z. Han and Z. Wang, *Chem.–Asian J.*,

2009, **4**, 32–41; (*d*) V. B. Birman, A. L. Rheingold and K.-C. Lam, *Tetrahedron: Asymmetry*, 1999, **10**, 125–131.

4 (*a*) F. Ozawa, A. Kubo, Y. Matsumoto, T. Hayashi, E. Nishioka, K. Yanagi and K. Moriguchi, *Organometallics*, 1993, **12**, 4188–4196; (*b*) J.-H. Xie, H.-F. Duan, B.-M. Fan, X. Cheng, L.-X. Wang and Q.-L. Zhou, *Adv. Synth. Catal.*, 2004, **346**, 625–632.

5 (*a*) J.-H. Xie, L.-X. Wang, Y. Fu, S.-F. Zhu, B.-M. Fan, H.-F. Duan and Q.-L. Zhou, *J. Am. Chem. Soc.*, 2003, **125**, 4404–4405; (*b*) C. Liu, J.-H. Xie, Y.-L. Li, J.-Q. Chen and Q.-L. Zhou, *Angew. Chem., Int. Ed.*, 2013, **52**, 593–596.

6 B.-M. Fan, J.-H. Xie, S. Li, L.-X. Wang and Q.-L. Zhou, *Angew. Chem., Int. Ed.*, 2007, **46**, 1275–1277.

7 (*a*) X. Wang, Z. Han, Z. Wang and K. Ding, *Acc. Chem. Res.*, 2021, **54**, 668–684; (*b*) J. Zeng, W. Fang, B. Lin, G.-Q. Chen and X. Zhang, *Org. Lett.*, 2022, **24**, 869–874; (*c*) J.-W. Park, Z. Chen and V. M. Dong, *J. Am. Chem. Soc.*, 2016, **138**, 3310–3313; (*d*) S. G. Sethofer, S. T. Staben, O. Y. Hung and F. D. Toste, *Org. Lett.*, 2008, **10**, 4315–4318.

8 (*a*) J. M. Crawford and M. S. Sigman, *Synthesis*, 2019, **51**, 1021–1036; (*b*) Q. Peng, F. Duarte and R. S. Paton, *Chem. Soc. Rev.*, 2016, **45**, 6093–6107; (*c*) J.-P. Genet, T. Ayad and V. Ratovelomanana-Vidal, *Chem. Rev.*, 2014, **114**, 2824–2880.

9 (*a*) X.-H. Huo, J.-H. Xie, Q.-S. Wang and Q.-L. Zhou, *Adv. Synth. Catal.*, 2007, **349**, 2477–2484; (*b*) S. Li, J.-W. Zhang, X.-L. Li, D.-J. Cheng and B. Tan, *J. Am. Chem. Soc.*, 2016, **138**, 16561–16566; (*c*) G.-Q. Chen, B.-J. Lin, J.-M. Huang, L.-Y. Zhao, Q.-S. Chen, S.-P. Jia, Q. Yin and X. Zhang, *J. Am. Chem. Soc.*, 2018, **140**, 8064–8068; (*d*) A. J. Argüelles, S. Sun, B. G. Budaitis and P. Nagorny, *Angew. Chem., Int. Ed.*, 2018, **57**, 5325–5329; (*e*) L. Yin, J. Xing, Y. Wang, Y. Shen, T. Lu, T. Hayashi and X. Dou, *Angew. Chem., Int. Ed.*, 2019, **58**, 2474–2478; (*f*) Z. Zheng, Y. Cao, Q. Chong, Z. Han, J. Ding, C. Luo, Z. Wang, D. Zhu, Q.-L. Zhou and K. Ding, *J. Am. Chem. Soc.*, 2018, **140**, 10374–10381; (*g*) R. Zhang, S. Ge and J. Sun, *J. Am. Chem. Soc.*, 2021, **143**, 12445–12449.

10 (*a*) X. Chang, P.-L. Ma, H.-C. Chen, C.-Y. Li and P. Wang, *Angew. Chem., Int. Ed.*, 2020, **59**, 8937–8940; (*b*) K. Tamao, K. Nakamura, H. Ishii, S. Yamaguchi and M. Shiro, *J. Am. Chem. Soc.*, 1996, **118**, 12469–12470.

11 L. Yang, W.-Q. Xu, T. Liu, Y. Wu, B. Wang and P. Wang, *Chem. Commun.*, 2021, **57**, 13365–13368.

12 (*a*) J. E. Marcone and K. G. Moloy, *J. Am. Chem. Soc.*, 1998, **120**, 8527–8528; (*b*) K. J. Cavell, *Coord. Chem. Rev.*, 1996, **155**, 209–243; (*c*) P. Dierkes and P. W. N. M. van Leeuwen, *J. Chem. Soc., Dalton Trans.*, 1999, 1519–1530; (*d*) P. W. N. M. van Leeuwen, P. C. J. Kamer, J. N. H. Reek and P. Dierkes, *Chem. Rev.*, 2000, **100**, 2741–2770; (*e*) Z. Freixa and P. W. N. M. van Leeuwen, *Dalton Trans.*, 2003, 1890–1901.

13 (*a*) I. Ojima, R. J. Donovan and W. R. Shay, *J. Am. Chem. Soc.*, 1992, **114**, 6580–6582; (*b*) I. Ojima, A. T. Vu, S.-Y. Lee, J. V. McCullagh, A. C. Moralee, M. Fujiwara and T. H. Hoang, *J. Am. Chem. Soc.*, 2002, **124**, 9164–9174.

14 For selected reviews and examples: (*a*) P. Cao, B. Wang and X. Zhang, *J. Am. Chem. Soc.*, 2000, **122**, 6490–6491; (*b*) C. Aubert, O. Buisine and M. Malacria, *Chem. Rev.*, 2002, **102**, 813–834; (*c*) A. Marinetti, H. Jullien and A. Voituriez, *Chem. Soc. Rev.*, 2012, **41**, 4884–4908; (*d*) I. D. G. Watson and F. D. Toste, *Chem. Sci.*, 2012, **3**, 2899–2919; (*e*) S. E. Denmark and J. H.-C. Liu, *J. Am. Chem. Soc.*, 2007, **129**, 3737–3744; (*f*) V. Michelet, P. Y. Toullec and J.-P. Genêt, *Angew. Chem., Int. Ed.*, 2008, **47**, 4268–4315; (*g*) B. M. Trost, *Acc. Chem. Res.*, 1990, **23**, 34–42; (*h*) H.-Y. Jang and M. J. Krische, *J. Am. Chem. Soc.*, 2004, **126**, 7875–7880; (*i*) B. M. Trost and M. Lautens, *J. Am. Chem. Soc.*, 1985, **107**, 1781–1783; (*j*) K. H. Park, I. G. Jung, S. Y. Kim and Y. K. Chung, *Org. Lett.*, 2003, **5**, 4967–4970; (*k*) T. Nishimura, T. Kawamoto, M. Nagaosa, H. Kumamoto and T. Hayashi, *Angew. Chem., Int. Ed.*, 2010, **49**, 1638–1641.

15 For recent examples: (*a*) M. Dong, L. Qi, J. Qian, S. Yu and X. Tong, *J. Am. Chem. Soc.*, 2023, **145**, 1973–1981; (*b*) Z. Chen, Y.-F. Li, S.-Z. Tan, Q. Ouyang, Z.-C. Chen, W. Du and Y.-C. Chen, *Chem. Sci.*, 2022, **13**, 12433–12439; (*c*) E. Hayashi, N. Akiyama, K. Kakiuchi, T. Kawai and T. Morimoto, *Chem.–Asian J.*, 2023, **18**, e202201241; (*d*) S.-H. Hou, X. Yu, R. Zhang, C. Wagner and G. Dong, *J. Am. Chem. Soc.*, 2022, **144**, 22159–22169; (*e*) X. Han, Q. Gaignard-Gaillard, P. Retailleau, V. Gandon and A. Voituriez, *Chem. Commun.*, 2022, **58**, 3043–3046.

16 (*a*) T. Shi, G. Yin, X. Wang, Y. Xiong, Y. Peng, S. Li, Y. Zeng and Z. Wang, *Green Synth. Catal.*, 2023, **4**, 20–34; (*b*) V. Bhardwaj, D. Gumber, V. Abbot, S. Dhiman and P. Sharma, *RSC Adv.*, 2015, **5**, 15233–15266.

17 H. Chakrapani, C. Liu and R. A. Widenhoefer, *Org. Lett.*, 2003, **5**, 157–159.

18 (*a*) S. B. Duckett and R. N. Perutz, *Organometallics*, 1992, **11**, 90–98; (*b*) S. Sakaki, M. Sumimoto, M. Fukuhara, M. Sugimoto, H. Fujimoto and S. Matsuzaki, *Organometallics*, 2002, **21**, 3788–3802.

19 S. E. Denmark and A. Ambrosi, *Org. Process Res. Dev.*, 2015, **19**, 982–994.

20 (*a*) X. Zeng, *Chem. Rev.*, 2013, **113**, 6864–6900; (*b*) D. Troegel and J. Stohrer, *Coord. Chem. Rev.*, 2011, **255**, 1440–1459; (*c*) R. J. Hofmann, M. Vlatković and F. Wiesbrock, *Polymers*, 2017, **9**, 534.

21 During the preparation of this manuscript, the preparation of the diphosphine ligands was reported by Wang *et al*: P. Wang, Y. Wu, Spiro-dihydrobenzothiole diphosphine compound, and preparation method and application thereof, *Chinese Pat.*, CN114478632, 2009.